

An investigation on instantaneous local heat transfer coefficients in high-temperature fluidized beds—I. Experimental results

HONG-SHUN LI, REN-ZHANG QIAN,† WEN-DI HUANG and KAI-JUN BI

Department of Power Engineering, Huazhong University of Science and Technology, Wuhan, Hubei (Province) 430074, China

(Received 12 November 1992 and in final form on 20 May 1993)

Abstract—Experimental results are presented and analysed for instantaneous and time-averaged local surface temperatures and heat transfer coefficients around a water-cooled horizontal tube of 40 mm in outer diameter immersed in a 230 × 160 mm cross section high temperature fluidized bed. Such measurements are made using a specially-designed thin-film thermocouple probe. Silica sands with mean diameter of 0.662, 1.103 and 1.815 mm are used as bed materials. Measurements are taken over a wide temperature range from 270 to 1028°C.

INTRODUCTION

FLUIDIZED bed combustion is advanced for the utilization of all ranks of coal in an environmentally acceptable manner. A fundamental knowledge of heat transfer in high temperature fluidized beds is essential for proper design and optimization of such a combustor. Although a large number of experimental investigations have been conducted, a great majority of this work was performed at lower bed temperatures. The characters of bed-to-surface heat transfer and fluidization behavior at elevated temperature have been observed to be different from those at lower temperatures. Also there still exist a number of unanswered questions regarding the mechanism of heat transfer in fluidized beds. Instantaneous local heat transfer coefficients will provide detailed knowledge of importance to obtain further insight into these questions.

Mickley *et al.* [1] were the first to measure the instantaneous bed-to-surface heat transfer coefficients by using a thin platinum foil attached to a vertical tube and following its temperature changes. Subsequent workers, including Tuot and Clift [2], Fitzgerald *et al.* [3], Wu *et al.* [4], Baskakov *et al.* [5], Gloski *et al.* [6], made use of thin-film technology with variations in the circuit used to power these devices. All of these investigations were conducted in low temperature fluidized beds. Few measurements of instantaneous local heat transfer coefficients in high temperature fluidized beds have been reported. George and Smalley [7] developed an instrumented cylinder for the measurement of instantaneous local heat flux around a horizontal tube in a fluidized bed at 743°C.

In order to measure instantaneous local heat transfer coefficients in high temperature fluidized beds, a thin-film thermocouple probe was developed in ref. [8], and was used to measure instantaneous local heat transfer coefficients around an immersed horizontal tube of 40 mm in outer diameter in a fluidized bed at 1034°C. Experiments reported here were carried out in fluidized beds of three bed materials with a temperature range of 270°C to above 1000°C. Details of experimental results are presented and analysed.

TEST RESULTS AND DISCUSSION

Thin-film thermocouple probe

The fabrication and operation procedures of the thin-film thermocouple probe have been described in detail in our previous publication [8]. In brief, as shown in Fig. 1, the probe consists of a constantan cylinder plug of 9 mm in diameter and 10 mm in length. A hole of 0.8 mm in diameter is drilled through the plug along the direction of its axis. One circular face of the plug is electroplated with a copper film of 50 μm thick, to which is attached an enamel-insulated copper wire of 0.5 mm in diameter, the copper wire is installed through the 0.8 mm diameter hole, and its side is insulated from the constantan plug. Another enamel-insulated copper wire (0.35 mm in diameter) is installed in the constantan plug at a distance of 6 mm from the copper film. The end of this copper wire contacts with the plug, but its side is insulated from the plug. A constantan wire of 0.2 mm in diameter is laser welded on the surface of the plug opposite to the copper film. Thus the probe has two sets of copper-constantan thermocouples giving the temperature of the copper film and that of the constantan at a point 6 mm away from the film. The output of the thermocouples is recorded on a computerized data acqui-

† Address correspondence to Prof. Ren-Zhang Qian.

NOMENCLATURE

d_p	mean particle diameter	$T_{s\theta}$	instantaneous local surface temperature at angular position θ
h_θ	instantaneous local heat transfer coefficient at angular position θ	$\bar{T}_{s\theta}$	time-average local surface temperature at angular position θ
$h_{\theta i}$	i th value of h_θ	u	gas velocity.
\bar{h}_θ	time-average local heat transfer coefficient at angular position θ	Greek symbol	
h_w	spatial-average heat transfer coefficient	θ	degree measured from lower stagnation point on the tube.
N	number of $h_{\theta i}$		
T_b	bed temperature		

sition system consisting of direct-current amplifier, 16 channel and 12 bit A/D convertor and IBM personal computer. The acquisition system is capable of measuring signals up to a frequency of 40 kHz. The thermal response time of the probe (i.e. time for the thin-film thermocouple to register 98% of a step change in surface temperature) is 2.57 ms. The copper film will become slowly thinner and thinner with use because of abrasion, thus the response time will be shorter and shorter. For example, when the copper film becomes 60 μm , 40 μm , 20 μm , the response time will be 1.45 ms, 0.65 ms, 0.16 ms respectively. Measured values of the two temperatures are employed as boundary condition to solve the one-dimensional unsteady heat conduction equation. From the solutions, the instantaneous local heat flux is obtained, thus instantaneous local heat transfer coefficients can be obtained. A single probe is installed in a 40 mm outer diameter and 20 mm inner diameter stainless steel tube, which is used as a section of a water-cooled immersed horizontal tube. The tube can be rotated so that data at all angular positions considered are taken.

Test conditions

The measurements are carried out in a high temperature fluidized bed. Lower required temperatures (less than 700°C) for heat transfer experiments are

achieved by burning diesel oil in an upstream combustion chamber and hot gas is directed into a 160 \times 230 mm cross test section. Higher temperatures (up to 1100°C) are obtained by burning diesel oil within the test section simultaneously. The distributor has 45 stainless steel bubble caps with an open area of 3.60%. The immersed tube is positioned horizontally in the test section, 230 mm above the distributor. Under each operating condition, the above mentioned data acquisition system is used to take 30 s of output signals of the thin-film thermocouple probe, with a recording speed of 125 Hz, for each of five angular positions ($\theta = 0, 45, 90, 135, 180^\circ$).

Test results

Figures 2 and 3 show typical instantaneous local surface temperatures and corresponding instantaneous local heat transfer coefficients for three different angular positions at a bed temperature of 1032°C, with the bed material of silica sand particles of 1.815 mm mean diameter. It can be seen that the bed-to-surface heat transfer is unsteady. Though instantaneous local surface temperatures fluctuate in a small range (less than 10%), the instantaneous local heat transfer coefficients may fluctuate in a large range of over 100%. Higher heat transfer coefficients imply a dense phase at the surface while the lower corresponds to a gas void at the surface. This phenomenon is represented quantitatively by void renewal frequency, which will be elaborated on in Part II of this paper.

From the instantaneous local heat transfer coefficient, the time-average local heat transfer coefficient, \bar{h}_θ , can be obtained

$$\bar{h}_\theta = \frac{1}{N} \sum_{i=1}^N h_{\theta i}. \quad (1)$$

The time-average heat transfer coefficient for the whole perimeter of the tube or spatial-average heat transfer coefficient present an overall picture of the changing hydrodynamic conditions within the immediate vicinity of the immersed tube, it is determined from \bar{h}_θ by the formula

$$h_w = (\bar{h}_{180} + 2\bar{h}_{135} + 2\bar{h}_{90} + 2\bar{h}_{45} + \bar{h}_0)/8. \quad (2)$$

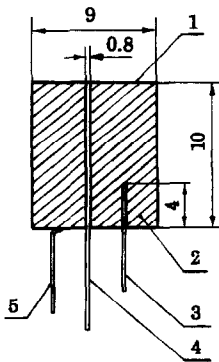


FIG. 1. Thin-film thermocouple probe (dimensions in mm). 1—copper film, 2—constantan, 3—copper wire, 4—copper wire, 5—constantan wire.

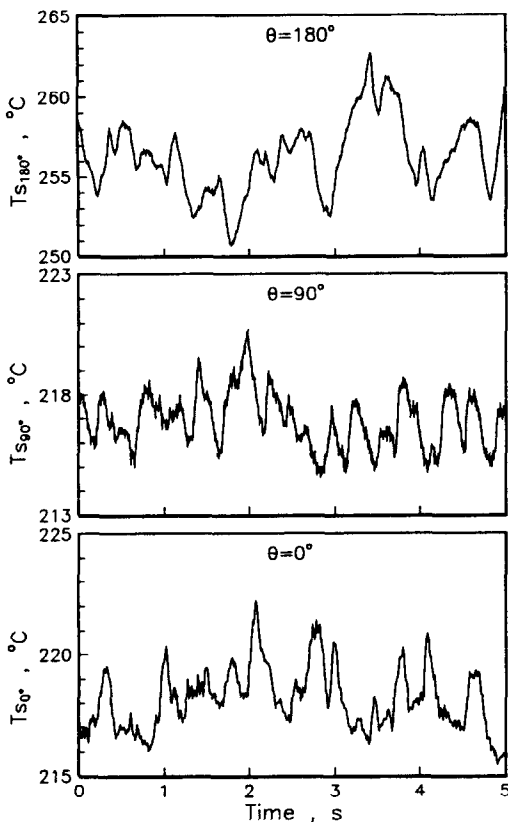


FIG. 2. Instantaneous local surface temperatures for $d_p = 1.815$ mm, $T_b = 1032^\circ\text{C}$, $u = 3.54$ m s $^{-1}$.

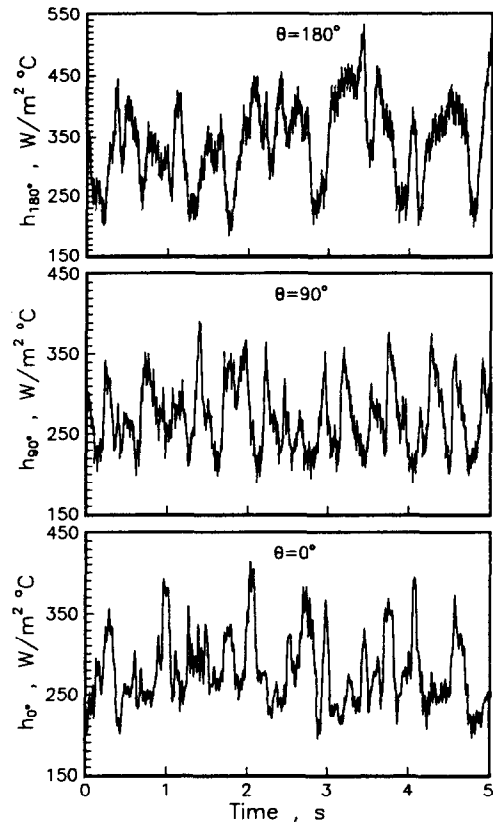


FIG. 3. Instantaneous local heat transfer coefficients for $d_p = 1.815$ mm, $T_b = 1032^\circ\text{C}$, $u = 3.54$ m s $^{-1}$.

Figure 4 shows the time-average local heat transfer coefficients for bed material of 1.815 mm mean diameter silica sand particles with variations in bed temperature. Similar data for 0.622 and 1.103 mm silica sand particles are not reproduced here for the sake of brevity but are discussed in the next paragraphs.

As can be seen, the time-average heat transfer coefficients vary significantly with changing gas velocity and changing angular position around the tube. For the bed of 1.815 mm mean diameter silica sand particles at 424°C (see Fig. 4(a)), the most obvious effects of gas velocity is the very large change in magnitude of the time-average local heat transfer coefficient at the upper stagnation point ($\theta = 180^\circ$ position) as the gas velocity is changed. At the lowest gas velocity indicated, the bed is not fluidized, the minimum time-average heat transfer coefficient is found at the upper stagnation point, while the maximum occurs at the lower stagnation point ($\theta = 0^\circ$ positions). Those results are consistent with the observations reported by George and Welty [9] and Goshayeshi *et al.* [10]. The temperature history record at the $\theta = 180^\circ$ position under this operating condition (see Fig. 1(a) in Part II of this paper) shows the instantaneous local surface temperature has little fluctuations and decreases gradually with time. This indicates the presence of a relatively cool unfluidized

stack of particles on the top of the tube. With increase in gas velocity, the time-average local heat transfer coefficient increases over the whole circumference, and the increase at the upper stagnation point of the tube is remarkable, the position of maximum coefficient shifts from the bottom of the tube ($\theta = 0^\circ$ position) to near the side of the tube. With further increase in gas velocity, the position of the maximum coefficient moves to the upper stagnation point ($\theta = 180^\circ$ position) of the tube.

It also can be seen from Fig. 4 that, the variations of time-average local heat transfer coefficients at 180° and 90° positions with gas velocity show a similar pattern, namely, two coefficients initially increase with increase in gas velocity, and then decrease slowly as gas velocity is increased further. But the variations of two coefficients are not synchronous, the coefficient at the 180° position lags behind the coefficient at the 90° position. However, the time-average local heat transfer coefficient at the 0° position approximately increases monotonously but slowly with increase in gas velocity. This complex variation is an indication that the local heat transfer mechanisms change significantly with varying fluidization states.

Mass fluxes of fluidizing gas at corresponding lowest gas velocities indicated separately in Figs. 4(a)–(e) are approximately equal. However, the dynamic

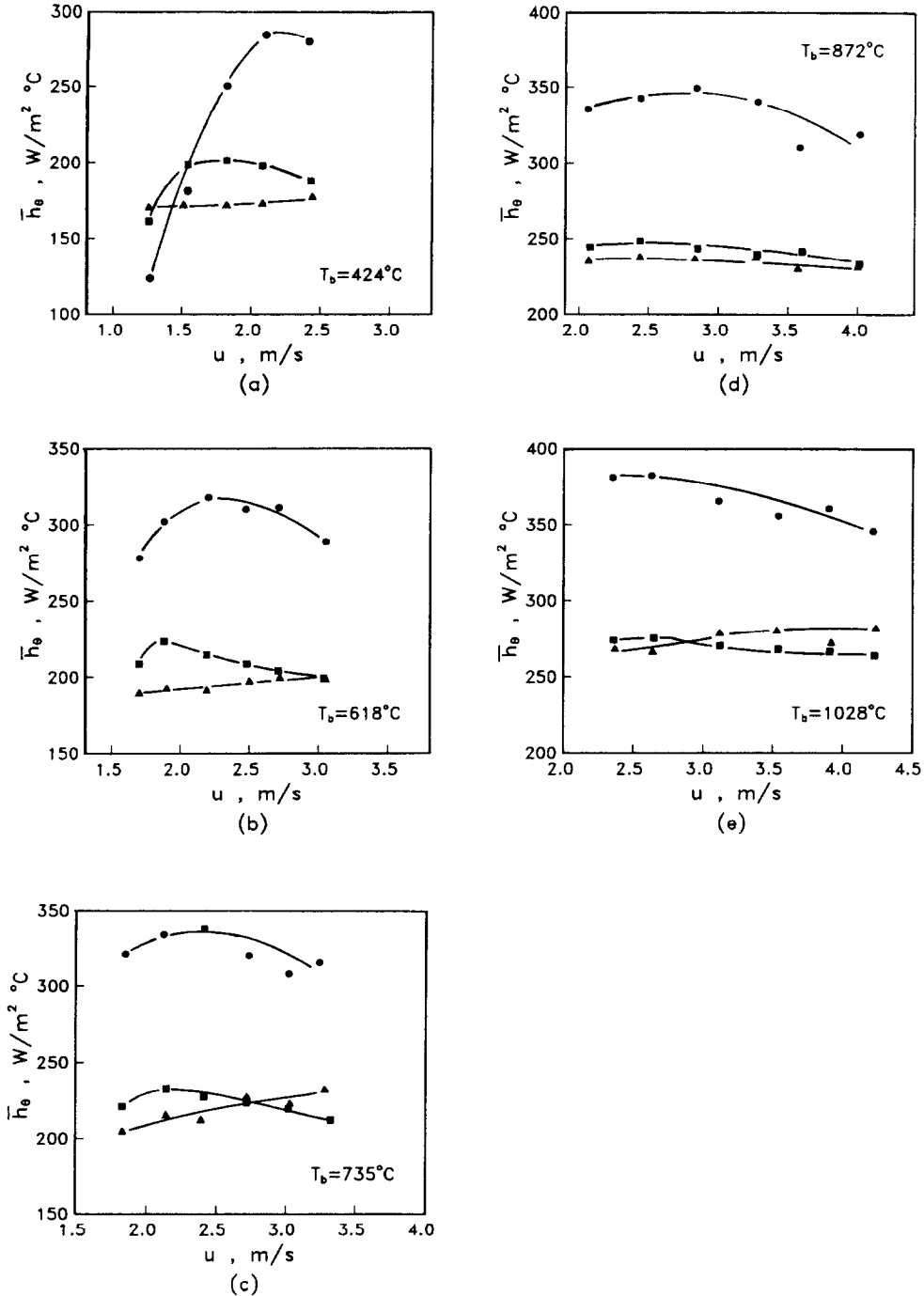


Fig. 4. Time-average local heat transfer coefficients for $d_p = 1.815$ mm. \bullet — $\theta = 180^\circ$, \blacksquare — $\theta = 90^\circ$, \blacktriangle — $\theta = 0^\circ$.

behaviors around the tube at the aforementioned gas velocities with variations in bed temperature are different. At a bed temperature of 424°C , as described above, there is a relatively cool unfluidized stack of particles on the top of the tube at the lowest velocity indicated. At higher temperatures, the time-average heat transfer coefficient at the 180° position is higher than that at the side and bottom of the tube, this

implies that the stack is removed. This phenomenon is due to the fact that particles and gas mix more violently when the temperature increases and results in the decrease in gas density which in turn increases gas velocity. This enhanced mix results in the disappearance of the unfluidized stack of particles.

Table 1 shows typical time-average local surface temperatures for the bed material of 1.815 mm mean

Table 1. Typical time-average local surface temperatures

θ (deg)	\bar{T}_{s0} (°C)				
	$T_b = 424^\circ\text{C}$ $u = 2.42 \text{ m s}^{-1}$	$T_b = 618^\circ\text{C}$ $u = 3.04 \text{ m s}^{-1}$	$T_b = 735^\circ\text{C}$ $u = 3.28 \text{ m s}^{-1}$	$T_b = 872^\circ\text{C}$ $u = 4.02 \text{ m s}^{-1}$	$T_b = 1028^\circ\text{C}$ $u = 4.21 \text{ m s}^{-1}$
180	113.8	153.7	177.4	213.5	249.5
135	104.4	131.1	156.5	194.8	224.5
90	94.5	124.6	151.2	179.0	213.3
45	89.1	119.5	150.3	178.9	218.3
0	87.5	120.1	149.7	174.4	218.7

diameter silica sand particles at each bed temperature. The bed is well fluidized at the operating conditions given in the table. For given test conditions, the time-average local surface temperature increases as the corresponding time-average local heat transfer coefficient increases. In the tested range of the gas velocity at a given bed temperature, most of time-average local surface temperatures change with gas velocity in a narrow range (less than 20°C).

coefficients for the three bed materials. Data were not obtained for the 0.622 mm mean diameter silica sand particles at about 1000°C because the oil gun inserted into the bed was plugged up by small particles during the operation. It is seen that at the lower bed temperatures, h_w initially has a relatively rapid increase as gas velocity is increased, becomes approximately constant, and then decreases slowly as gas velocity is further increased. By contrast, at the higher bed temperatures, such decreases in h_w with gas velocity

Figures 5–7 show spatial-average heat transfer

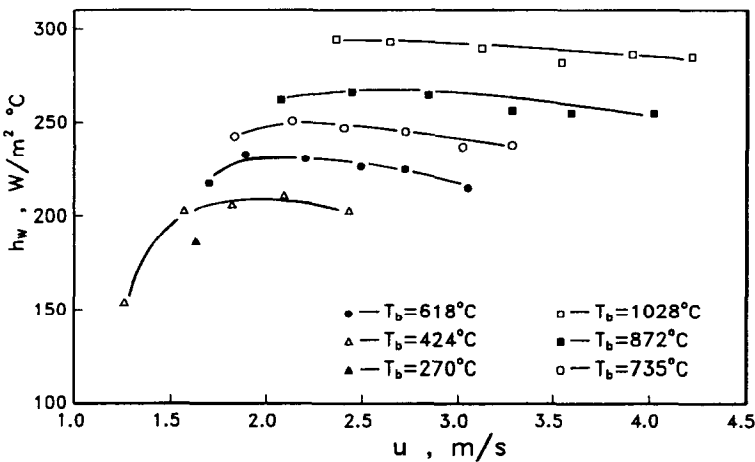


FIG. 5. Spatial-average heat transfer coefficients for $d_p = 1.815 \text{ mm}$.

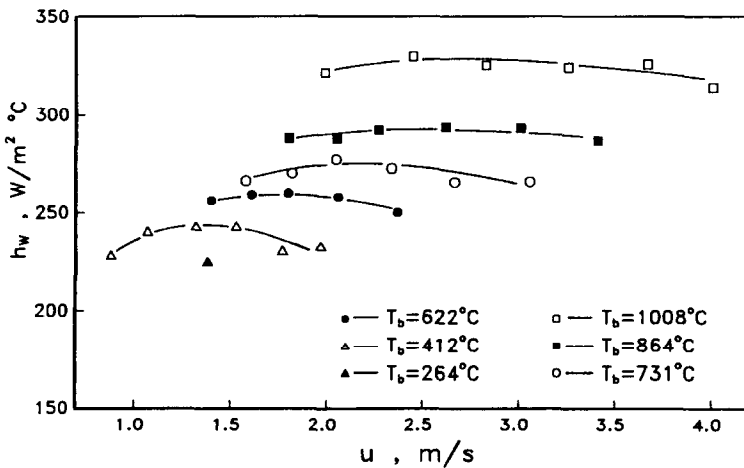


FIG. 6. Spatial-average heat transfer coefficients for $d_p = 1.103 \text{ mm}$.

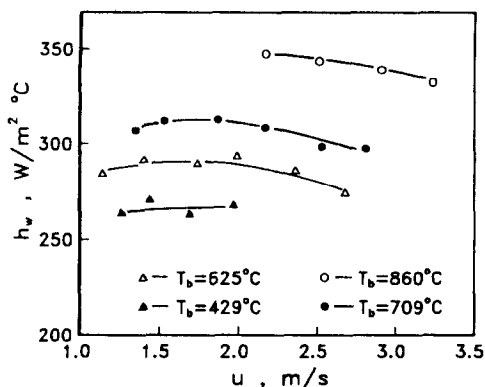


FIG. 7. Spatial-average heat transfer coefficients for $d_p = 0.622$ mm.

becomes slower. This can be attributed to the contribution of the radiant heat transfer between the bed and the tube, which increases continuously with increase in bed temperature. This variation of h_w with gas velocity indicates that once the bed is well fluidized, further increase in gas velocity has only marginal effect on h_w .

Figure 8 plots the variation of h_w as a function of bed temperature for the three bed materials. It is seen that h_w increases with increase in bed temperature. Moreover, there is a slight exponential relationship between h_w and the bed temperature within the range of the temperature investigated. This can be attributed to two sources: to the contribution of radiant heat transfer, which increases continuously with increase in bed temperature, and to the change in thermal properties of the fluidizing gas. Increased gas thermal conductivity with increased temperature enhances the conductance of the gas film between the tube and particles and, therefore, increases the emulsion phase convective and bubble phase convective contributions to the overall heat transfer coefficient.

Also it can be seen from Fig. 8 that h_w is significantly influenced by the particle size under certain operating

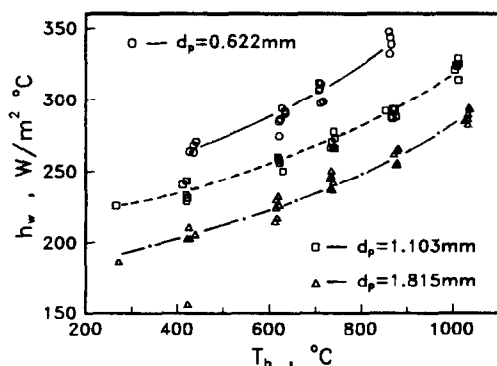


FIG. 8. Variation of h_w with T_b .

conditions, h_w increases with decreasing particle size. This behavior can be explained as predominantly due to an increase in the average gas conduction paths between the heat transfer tube and the first row of particles and between particles. The increase in conduction path increases the resistance to heat flow. Further, the number of particles contacting with the per unit tube surface is more for small particles, thus small particles are more efficient in exchanging heat with the tube.

CONCLUSIONS

In this investigation, the measured instantaneous local heat transfer coefficients and their corresponding time-average and spacial-average values for an immersed horizontal tube as a function of bed temperatures, fluidizing gas velocity and particle diameter have been presented. Based on this study, the conclusions can be drawn as follows.

(a) The heat transfer process in high temperature fluidized beds is found to be unsteady, the instantaneous local heat transfer coefficient fluctuates by over 100%.

(b) Time-average local heat transfer coefficients around an immersed horizontal tube are significantly different for different circumferential positions. Under packed bed condition, the position of the maximum local heat transfer occurs at the lower stagnation point, under the well fluidized state, the position moves to the upper stagnation point of the tube.

(c) The time-average local heat transfer coefficients at upper stagnation point and the side (90° position) of the tube are found to increase initially with increase in gas velocity, and then slightly decrease as gas velocity increases further. Whereas the time-average local heat transfer coefficients at the lower stagnation point of the tube are found to continuously but more slowly increase as gas velocity increases.

(d) Bed temperature has a significant effect on the fluidizing state of the bed. At the same fluidizing gas mass flux, the bed becomes more turbulent with increase in bed temperature.

(e) h_w increases with increase in bed temperature on a slight exponential relationship.

(f) h_w decreases with an increase in particle size from 0.622 to 1.815 mm.

REFERENCES

1. H. S. Mickley, D. F. Fairbanks and R. D. Hawthorn, The relation between the transfer coefficient and thermal fluctuations in fluidized-bed heat transfer, *Chem. Engng Prog. Symp. Ser.* **57**(32), 51-60 (1961).
2. J. Tuot and R. Clift, Heat transfer around single bubble in a two-dimensional fluidized bed, *A.I.Ch.E. Symp. Ser.* **69**(128), 78-84 (1973).
3. T. J. Fitzgerald, N. M. Catipovic and G. N. Jovanovic, Instrumented cylinder for studying heat transfer to immersed tubes in fluidized beds, *Ind. Engng Chem. Fundam.* **20**, 82-88 (1981).

4. R. L. Wu, C. J. Lim and J. R. Grace, The measurement of instantaneous local heat transfer coefficients in a circulating fluidized bed, *Can. J. Chem. Engng* **67**, 301–307 (1989).
5. A. P. Baskakov, N. F. Filippovskiy, A. A. Zhakov and L. V. Kotova, Investigation of fluctuation of the heat transfer coefficients in fluidized and pulsed beds. *Heat Transfer—Sov. Res.* **14**, 102–106 (1982).
6. D. Gloski, L. Glicksman and N. Decker, Thermal resistance at a surface in contact with fluidized bed particles, *Int. J. Heat Mass Transfer* **27**, 599–610 (1984).
7. A. H. George and J. L. Smalley, An instrumented cylinder for the measurement of instantaneous local heat flux in high temperature fluidized beds, *Int. J. Heat Mass Transfer* **34**, 3025–3036 (1991).
8. Hong-Shun Li, Kai-Jun Bi, Wen-Di Huang and Ren-Zhang Qian, A probe for the measurement of instantaneous local heat transfer coefficients around a horizontal immersed tube in a high temperature fluidized bed (in Chinese), *Proc. of Symp. on Heat and Mass Transfer*, Chinese Society of Engineering Thermophysics, Yantan, China, Vol. 2, Session VI, pp. 21–26 (1991).
9. A. H. George and J. R. Welty, Local heat transfer coefficients for a horizontal tube in a large-particle fluidized bed at elevated temperature, *A.I.Ch.E. JI* **30**, 482–485 (1984).
10. A. Goshayeshi, J. R. Welty, R. L. Adams and N. Alavizadeh, Local heat transfer coefficients for horizontal tube arrays in high temperature large particle fluidized beds—an experimental study, *J. Heat Transfer* **108**, 907–913 (1987).